Electronic Structure of a Paramagnetic {MNO}[superscript 6] Complex: MnNO 5,5-Tropocoronand

Electronic Structure of a Paramagnetic $\{MNO\}^6$ Complex: MnNO 5,5-Tropocoronand

Espen Tangen,[a] Jeanet Conradie,[a,b] Katherine Franz,[c] Simone Friedle,[c] Joshua Telser,*[d] Stephen J. Lippard,*[c] and Abhik Ghosh*[a]

[a] Department of Chemistry and Center for Theoretical and Computational Chemistry, University of Tromsø, N-9037 Tromsø, Norway

[b] Department of Chemistry, University of the Free State, 9300 Bloemfontein, Republic of South Africa

[c] Department of Chemistry, Massachusetts Institute of Technology, Cambridge, Massachusetts 02139

[d] Department of Biological, Chemical, and Physical Sciences, Roosevelt University, Chicago, Illinois 60605, USA

* Correspondence authors: AG abhik.ghosh@uit.no; SJL lippard@mit.edu;

JT jtelser@roosevelt.edu.

Keywords: manganese, tropocoronand, nitrosyl

Abstract. Using DFT (OLYP/STO-TZP) calculations, we have investigated the electronic structure of [Mn(5,5-tropocoronand)(NO)], a rare paramagnetic $\{MNO\}^6$ complex. Experimental methods, including magnetic susceptibility measurements and HFEPR spectroscopy, have not provided an unambiguous spin state assignment for this complex. In other respects, however, the compound was fully characterized, including by means of single-crystal X-ray structure determination. The optimized $S = 1$ OLYP geometry reproduced all key aspects of the trigonal-bipyramidal molecular structure, including a short Mn-N(O) distance (~1.7 Å) and an essentially linear MnNO angle. In contrast, the $S = 0$ and $S = 2$ optimized structures disagreed with the crystal structure in critical respects. Moreover, three different exchange-correlation functionals (OLYP, B3LYP, and B3LYP*) indicated an $S = 1$ ground state by a clear margin of energy. An examination of the Kohn-Sham MOs of this state indicated a primarily $d_{xz}^2 d_{yz}^2 d_{xy}^1 d_{x2-z2}^1$ electronic configuration, where the z axis is identified with the nearly linear MnNO axis. The d_{y2} orbital is formally unoccupied in this state, interacting, as it does, head-on with two tropocoronand nitrogens lying along the y axis, the pseudo-threefold axis of the trigonal-bipyramid. The doubly occupied d_{xz} and d_{yz} orbitals are in actuality d_π(Fe)-π^*(NO)-based π-bonding molecular orbitals, the α and β "components" of which are significantly offset spatially. This offset results in excess minority spin density on the NO unit. Thus, the OLYP/TZP atomic spin populations are: Mn 2.85, N(O) -0.52 and O -0.35.

Introduction

The biological importance of NO[1,2,3,4,5] and the many subtleties of transition metal-NO bonding continue to inspire fundamental studies of nitrosyl complexes, including numerous electronic structure calculations.[6] With the advent of density functional theory (DFT)[7,8] methods in chemistry some two decades ago and especially over the last decade, many aspects of transition metal nitrosyls have been studied in great detail,[6] relative to what was possible with semiempirical methods.[9,10] Compared with metalloporphyrin-NO electronic structures,[11] however, the more electronically diverse nonheme nitrosyls have been less thoroughly explored with DFT methods.[12,13] As part of our ongoing efforts to explore the latter area,[14,15,16,17,18,19] we carried out a DFT study of an MnNO tropocoronand complex, [Mn(5,5-TC)(NO)],[20] which was reported in the course of an extensive series of studies of complexes of this ligand.[21] The structure of the free ligand, H_2TC-n,m, and its numbering scheme are shown in Chart 1. Given the dianionic nature of the 5,5-TC ligand, neutral [Mn(5,5-TC)(NO)] can be formally considered as any of the three extreme forms, [Mn^{III}-NO^-], [Mn^{II}-$NO^{\cdot}$], or [Mn^{I}-NO^+], collectively represented as $\{MnNO\}^6$ in the Enemark-Feltham notation.[10] The striking property of this complex is its paramagnetism. Thus $\{MNO\}^6$ metalloporphyrin derivatives are invariably diamagnetic and, for nonheme systems, we are aware of only one other example of a paramagnetic $\{MNO\}^6$ complex, Fe(PS_3)(NO), where PS3 is a tris(thiolato)phosphine ligand.[15] Although [Mn(5,5-TC)(NO)] has been well-characterized experimentally,[20] a theoretical description of its electronic structure has not yet been reported. Here we provide such a description based on DFT calculations.

Computational methods

The DFT studies were carried out with the OLYP[22,23] functional, all-electron STO-TZP basis sets, fine grids for numerical integration of matrix elements, tight SCF and geometry optimization criteria, and a spin-unrestricted formalism, all as implemented in the ADF 2007 program system.[24]

Magnetic analysis methods

Magnetic susceptibility data recorded previously were refit with a locally written program (available from J. Telser) that involved solving a standard spin Hamiltonian matrix for $S = 1$ or 2, which included the electronic Zeeman effect, $\mathcal{H}_{\mathrm{elZ}} = \beta_e B \bullet \mathbf{g} \bullet S$, and zero-field splitting (zfs), defined as $\mathcal{H}_{\mathrm{zfs}} = S \bullet \mathbf{D} \bullet S$. Higher-order zfs terms and any intermolecular interactions are disregarded in this approach.[25] The program sums several hundred molecular orientations with respect to the external magnetic field to achieve a true powder pattern averaged magnetic susceptibility. Non-linear least-squares fitting yields the optimal parameters within certain constraints. The parameter space is potentially large and only interactions that have a significant effect are included. Thus, only isotropic or axial g values were employed, i.e., not rhombic, and only axial zfs was included ($D \neq 0$, $E \equiv 0$). Magnetic susceptibility has difficulty in determining of the sign of D, thus fits constrained to both positive and negative values were employed. Lastly, temperature independent paramagnetism (TIP) was included to model crudely the effect of excited states not accounted for by the simple $S = 1$ or 2 spin Hamiltonian.[26] Experimentally, TIP models the upward slope in the μ_{eff} value at higher temperature, without the TIP value becoming unreasonably large ($> 10^{-2}$).

Results and discussion

(a) Magnetic and spectroscopic studies. Experimentally, [Mn(5,5-TC)(NO)] is paramagnetic and the original analysis of the magnetic susceptibility measurements appeared to indicate an $S = 2$ spin ground state. As part of this study, we reanalyzed the magnetic data for this complex in more detail, using an exact calculation method rather than the analytical method originally employed.[20] Nevertheless, the original fit results emerged unmolested from the more exact treatment. Table 1 summarizes the current and previous fit results.

Table 1. Summary of fits to the magnetic susceptibility data for [Mn(5,5-TC)(NO)]

Fit model	***D* (cm^{-1})**	***g***	**TIP**
$S = 1, D \geq 0, g_{iso}$	+6.4	2.70	2.3 x 10^{-3}
$S = 1, D \leq 0, g_{iso}$	-10.2	2.75	1.5 x 10^{-3}
$S = 1, D \leq 0, g_{ax}$ [a]	-6.2	3.07 (*xy*), 2.06 (*z*)	1.3 x 10^{-3}
$S = 1$, D free, g_{ax} [a]	-8.2	2.87 (*xy*), 2.51 (*z*)	1.4 x 10^{-3}
$S = 1$ [b]	6.4	2.7	---
$S = 2, D \geq 0, g_{iso}$	+5.8	1.59	1.3 x 10^{-3}
$S = 2, D \leq 0, g_{iso}$	-5.1	1.59	1.5 x 10^{-3}
$S = 2, D \geq 0, g_{ax}$	+6.2	1.61 (*xy*), 1.47 (*z*)	1.8 x 10^{-3}
$S = 2, D \leq 0, g_{ax}$	-3.9	1.65 (*xy*), 1.52 (*z*)	1.1 x 10^{-3}
$S = 2$, D free, g_{ax}	+6.1	1.61 (*xy*), 1.50 (*z*)	1.7 x 10^{-3}
$S = 2$ [b]	5.6	1.6	---

[a] With g_{ax} ($g_y \equiv g_x \neq g_z$), the fit tends to drive $D < 0$.

[b] ref 20.

Clearly, the original fit results are valid. Qualitatively, the $S = 1$ model yields g values that are larger than are expected for Mn(III), whereas the $S = 2$ model yields values that are lower than expected.[27,28,29,30] It is difficult to draw any further conclusions from the fit

parameters with respect to zfs. The magnitude of D, regardless of fit, is larger than is typically found for five-coordinate, albeit square-pyramidal rather than TBP, Mn(III). As is generally the case for variable temperature magnetic susceptibility studies, the sign of D cannot be determined. This sign is usually negative for high-spin Mn(III), but such was not the case in a diiodo complex, where spin-orbit coupling contributions to D from, effectively, I· were important.[31] Thus, a noninnocent ligand, albeit made of light atoms with small free-ion spin-orbit coupling, might conceivably lead to unusual zfs, and there are no good analogs to [Mn(5,5-TC)(NO)].

Given that high-frequency high-field electron paramagnetic resonance (HFEPR) has been successfully applied to a variety of Mn(III) complexes,[27-31,32,33,34] we applied this technique to a freshly prepared sample of [Mn(5,5-TC)(NO)]. The HFEPR spectrometer of the EMR facility of the National High Magnetic Field Laboratory (NHMFL, Tallahassee, Florida) was employed, an instrument that has been described elsewhere.[35] Unfortunately, the results were inconclusive and it was impossible to extract spin Hamiltonian parameters from the recorded spectra or even to assign a spin ground state (temperatures of ~5 K were employed for HFEPR). All that could be concluded from the HFEPR studies is that the complex has an integer-spin (non-Kramers) ground state and that there is essentially no evidence for the presence of any half-integer (Kramers) systems such as Mn(II), Mn(IV), or spin-coupled systems with total S = 1/2, 3/2, 5/2, etc. This latter point is in agreement with the conventional EPR-silence of [Mn(5,5-TC)(NO)] noted earlier.[20]

Given that neither the S = 1 nor the S = 2 models yielded satisfactory fit parameters for the magnetic susceptibility data and that it also proved impossible to extract such parameters by HFEPR, we cannot make an unequivocal experimental determination of the ground spin-state of Mn(5,5-TC)(NO)], except that it is clearly paramagnetic, which is

striking for an {MNO}^{6} system. DFT calculations, however, shed light on this problem, as described next.

(b) DFT calculations. In view of the ambiguity of the magnetic and spectroscopic studies, we chose to optimize all three relevant spin states, i.e. $S = 0$, 1, and 2. Key results of these OLYP/TZP calculations are presented in Figure 1, including selected geometry parameters, Mulliken spin populations, and spin density plots. Single-point energies were also determined for the three spin ground states with the B3LYP (20% Hartree-Fock exchange) and B3LYP* (15% Hartree-Fock exchange) hybrid functionals and these are listed in Table 2.

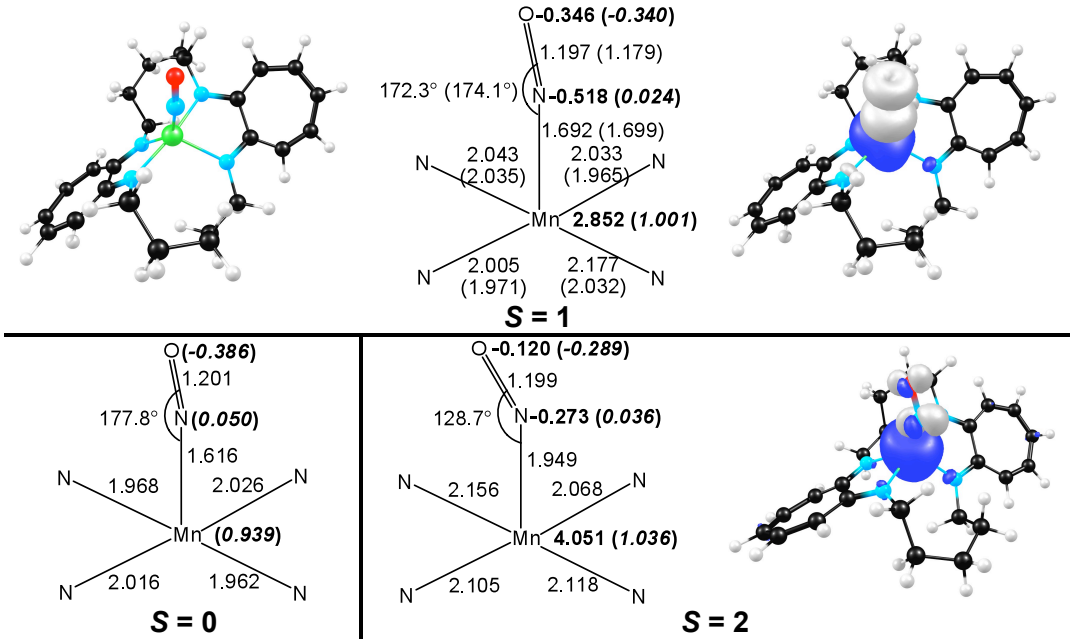

Figure 1. Selected OLYP/TZP optimized geometry parameters (Å, deg), Mulliken spin populations (bold) and charges (bold italics in parentheses) for different states of [Mn(5,5-TC)(NO)]. For the spin density plots (contour 0.04 e/Å^3) , majority and minority spin densities are indicated in blue and grey, respectively.

Table 2. DFT spin state energies (eV) of [Mn(5,5-TC)(NO)] and Fe(PS3)(NO) relative to the $S = 1$ state as zero level in each case.

	[Mn(5,5-TC)(NO)]			Fe(PS3)(NO)
S	OLYP	B3LYP*	B3LYP	OLYP
0	0.26	0.45	0.68	0.45
1	**0.00**	**0.00**	**0.00**	**0.00**
2	0.68	0.59	0.43	1.19

The optimized geometries for all three spin states may be described as trigonal-bipyramidal with the NO in an equatorial position (TBP_{eq}), consistent with the crystal structure of [Mn(5,5-TC)(NO)]. Such a structure follows straightforwardly from the inherent steric requirements of the 5,5-TC ligand, which also forms a number of other TBP_{eq} complexes.[21] Experimentally, [Mn(5,5-TC)(NO)] has a nearly linear NO unit, with an Mn–N–O angle of 174.1°, and Mn–N(O) and N–O distances of 1.699(3) and 1.179(3) Å, respectively.[20] As shown in Figure 1, only the optimized $S = 1$ structure exhibits geometry parameters that closely agree with these values. Thus, whereas the optimized Mn–N(O) distance is 1.692 Å for the $S = 1$ state, in near-perfect agreement with the crystal structure,[20] it is too short (1.616 Å) for $S = 0$ and too long (1.949 Å) for $S = 2$. Moreover, although both the $S = 0$ and $S = 1$ optimized structures feature nearly linear Mn–N–O units, the $S = 2$ structure has a strongly bent NO (Mn–N–O angle: 128.7°), which is clearly at odds with the crystal structure. These geometrical correlations strongly suggest that [Mn(5,5-TC)(NO)] has an $S = 1$ ground state.

The DFT energetics results (Table 2) are also consistent with the above state assignment. Relative to the $S = 1$ state as zero level, the energy of the lowest $S = 0$ state is +0.26 eV with OLYP, +0.45 eV with B3LYP* and +0.68 eV with B3LYP. The $S = 2$ state is also higher in energy: +0.68 eV with OLYP, +0.59 eV with B3LYP* and +0.43 eV with

B3LYP, all relative to the $S = 1$ ground state. The overall pattern of the calculated spin state energetics is consistent with our previous observations; viz. pure functionals in general favor a more spin-coupled, covalent description, whereas hybrid functionals behave oppositely.17,18,36,37 The newer OLYP functional is better in this respect than classic pure functionals such as PW91 or BP86; B3LYP*, in certain cases, appears to be better than B3LYP.[17,38,39,40] All three functionals concur, however, in indicating an $S = 1$ ground state by a clear margin of energy.

(c) Molecular orbital considerations. To interpret the above results in terms of a molecular orbital picture, we present d-orbital energy level diagrams for $S = 1$ [Mn(5,5-TC)(NO)], its $S = 1/2$ iron analogue [Fe(5,5-TC)(NO)], and Fe(PS3)(NO) in Figure 2. Somewhat more detailed, but perhaps less reader-friendly, versions of these diagrams are presented in Figures S1-S3 in the Supporting Information. As noted earlier for [Fe(5,5-TC)(NO)],[19] an opposing pair of tropocoronand nitrogen atoms create the strongest ligand field along the pseudo-C_3 axis of the trigonal bipyramid; the d-orbital aligned along this axis, which we designate d_{y2}, is thus the highest in energy and is unoccupied for both [Mn(5,5-TC)(NO)] and [Fe(5,5-TC)(NO)]. The metal-NO(π^*) π-bonding MOs, based on the d_{xz} and d_{yz} orbitals (which may also be referred to as d_{π} and $d_{\pi'}$) in our coordinate system, are then the lowest-energy d orbitals. These two orbitals are doubly occupied for both [Mn(5,5-TC)(NO)] and [Fe(5,5-TC)(NO)]. The d_{xy} and d_{x2-z2} orbitals are intermediate in energy, with the latter, which has a lobe pointing directly at the NO, slightly higher in energy than the former. The d-electron configuration of [Mn(5,5-TC)(NO)] is therefore described as $d_{\pi}^2 d_{\pi}^2 d_{xy}^1 d_{x2-z2}^1$ and that of [Fe(5,5-TC)(NO)] as $d_{\pi}^2 d_{\pi}^2 d_{xy}^2 d_{x2-z2}^1$.

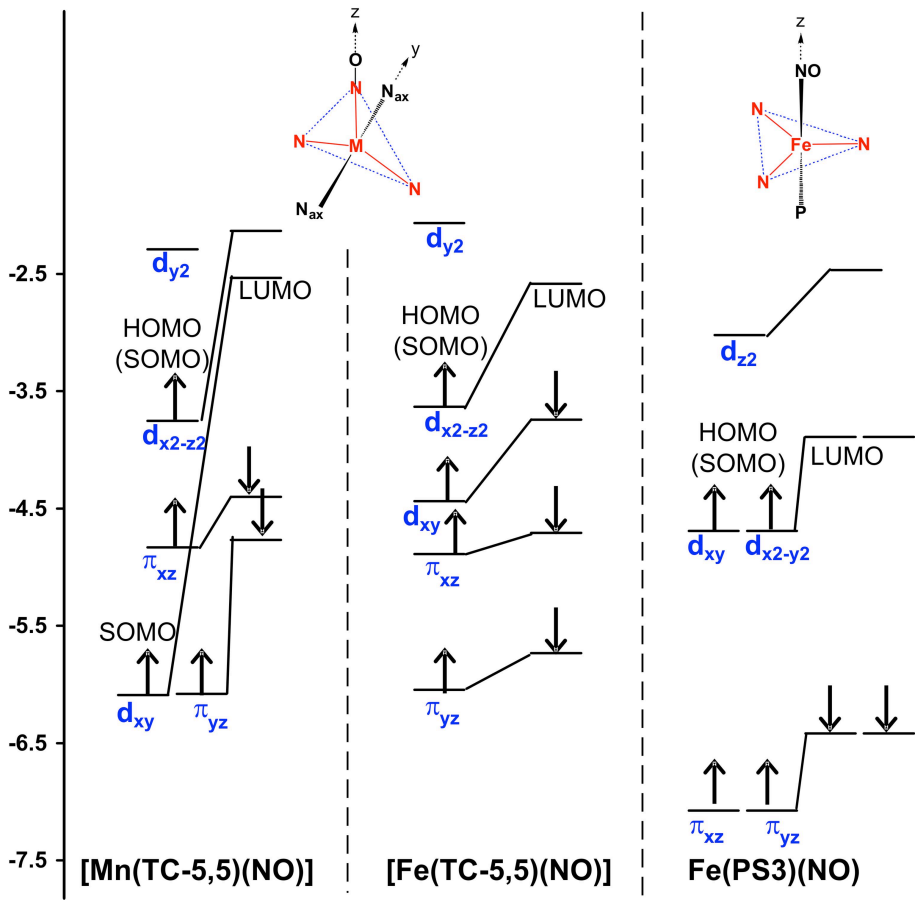

Figure 2. OLYP/TZP d-orbital-based MO Kohn-Sham energy (eV) levels for [Mn(5,5-TC)(NO)] (S = 1), [Fe(5,5-TC)(NO)] (S = 1/2) and Fe(PS3)(NO) (S = 1). For constructing this diagram (but not elsewhere in the paper), we have assumed C_2 symmetry for the two 5,5-TC complexes and C_{3v} symmetry for Fe(PS3)(NO). Energy levels for primarily ligand-based MOs are not shown here, but they are indicated in Figures S1 - S3 (Supporting Information).

Some of us have proposed earlier that the detailed topology of the occupied d_{π} orbital, the d_{x2-z2} orbital in this case, controls the MNO angle.[15,16,19] A half-occupied d_{z2} orbital such as that found in heme-based $\{FeNO\}^7$ complexes is highly stereochemically active. However, when admixed with metal p_z character as in certain nonheme complexes, the d_{z2}-p_z hybrid orbital is much less stereochemically active, resulting in a linear MNO fragment. For the 5,5-TC complex, the d_{x2-z2} orbital is similarly less stereochemically active than a typical d_{z2} orbital, which protrudes further into space; this feature provides a rationale for the essentially linear MNO groups in both [Mn(5,5-TC)(NO)] and [Fe(5,5-TC)(NO)].

Although useful for explanatory purposes, the above simple picture is clearly an approximate one. As shown in Figure 1 and Table 2, the $S = 1$ ground state of [Mn(5,5-TC)(NO)] exhibits substantial broken-symmetry character, i.e., spatial separation of majority and minority spin densities. An examination of the molecular orbitals clearly reveals that this feature, not unusual for transition metal nitrosyls, results from a spatial offset between the majority-spin and minority-spin metal-MO π-bonding orbitals, the latter being much more polarized toward the NO units relative to the former. The cylindrically symmetric minority spin density on the NO may thus be taken as indicative of an essentially [Mn^{III}($S = 2$)–NO^{-}($S = 1$)] description, which is analogous to the [Fe^{III}($S = 3/2$)–NO^{-}($S = 1$)] description proposed for [Fe(5,5-TC)(NO)]. Note that because the d_{y2} orbital is unoccupied, our calculations clearly rule out a high-spin Mn(II) center or, for that matter, high-spin Fe(II) and Fe(III centers. Qualitatively, this finding may be related to the dissimilarity in approximate zfs parameters between [Mn(5,5-TC)(NO)] and nonnitrosyl Mn(III) complexes. The broken-symmetry mature of this complex may also translate to an S intermediate between 1 and 2 in the spin Hamiltonian formalism, which would provide a rationale for the unusual g values mentioned above.

Table 3. Mulliken spin populations for the lowest $S = 1$ and $S = 2$ states of [Mn(5,5-TC)(NO)] for three different functionals.

	OLYP			B3LYP*			B3LYP		
S	Mn	N	O	Mn	N	O	Mn	N	O
1	2.852	-0.518	-0.346	3.036	-0.637	-0.455	3.182	-0.714	-0.507
2	4.051	-0.273	-0.12	4.132	-0.304	-0.118	4.227	-0.351	-0.129

It is instructive to compare the electronic structures of [Mn(5,5-TC)(NO)] and Fe(PS3)(NO), which are remarkably similar in some respects. Both are TBP complexes with strong-field ligands; the NO, however, is at an equatorial site in the former complex and at an apical site in the latter. Both have triplet ground states. The triplet ground states are readily rationalized in terms of two relatively low-energy, doubly occupied d_{π}-p_{π} bonding MOs and one high-energy d orbital aligned along the direction of the strongest ligand field, which leaves two singly occupied d orbitals in each case. As shown in Figure 2, the two "SOMOs" – using the term in a loose sense, given that the calculations are spin-unrestricted – are exactly degenerate for C_{3v}-symmetric Fe(PS3)(NO) and relatively similar in energy for [Mn(5,5-TC)(NO)], suggesting that there should be a moderately low-energy $S = 0$ state for each of the two complexes. As indicated in Table 2, explicit calculations confirm this hypothesis. However, the lowest $S = 2$ state is considerably higher in energy for Fe(PS3)(NO) than it is for [Mn(5,5-TC)(NO)].

Conclusions. [Mn(5,5-TC))NO] is a rare example of a paramagnetic $\{MNO\}^6$ complex. In view of inconclusive results from magnetic measurements and HFEPR spectroscopy, which could not distinguish between $S = 1$ and $S = 2$ ground states, we carried out a DFT study of the [Mn(5,5-TC)(NO)]. Our calculations clearly indicate an $S = 1$ ground

state. The optimized $S = 1$ geometry agrees well with the crystal structure, whereas the $S = 0$ and $S = 2$ geometries do not. The electronic structure is reasonably similar to that of $S = 1/2$ [Fe(5,5-TC)NO]. For both complexes, the d_{y2} orbital, which points toward a pair of antipodal tropocoronand nitrogen atoms (located along the pseudo-C_3 axis of the complex), is unoccupied. Both complexes also feature a pair of doubly occupied metal(d_σ)-NO(π^*) orbitals. For [Mn(5,5-TC)(NO)], this assignment leaves a pair of singly occupied d orbitals, which are the d_{xy} and d_{x2-z2} orbitals in our coordinate system where the NO ligand is roughly along the z axis.

On a broader note, while pursuing our interest in electronic-structural rarities, particularly unusual NO complexes,[6] we have been rewarded with unexpectedly general insights. Perhaps the most intriguing of these is the apparent relation between the precise topology of the d_σ orbital and the linearity or otherwise of the NO unit in nonheme NO complexes. Another interesting finding is the significant spatial separation of majority and minority spin densities, which appears to be a ubiquitous feature of open-shell nonheme NO complexes. Clear experimental verification of this phenomenon is yet to emerge, but we suspect that it may be account for the difficulties we have experienced with both analyzing the magnetometric data and obtaining the EPR spectra for [Mn(5,5-TC)(NO)].

Acknowledgements. This work was supported by the Research Council of Norway (AG), the National Science Foundation (SJL), and the South African National Research Foundation (JC). The HFEPR studies were supported by the NHMFL, which is funded by the NSF through Cooperative Agreement DMR 0654118, the State of Florida, the DOE. J.T. acknowledges NHMFL UCGP 5062 and we thank Drs. J. Krzystek and A. Ozarowski (NHMFL) for assistance with the HFEPR experiments.

Supporting Information Available: Optimized Cartesian coordinates for selected systems, MO energy level diagrams, magnetic susceptibility data and fits. This information is available free of charge via the Internet at http://pubs.acs.org.

References

1. (a) Murad, F. *Angew. Chem., Int. Ed.* **1999**, *38*, 1856-1868. (b) Furchgott, R. F. *Angew. Chem., Int. Ed.* **1999**, *38*, 1870-1880. (c) Ignarro, L. J. *Angew. Chem., Int. Ed.* **1999**, *38*, 1882-1892.

2. Westcott, B. L.; Enemark, J. L. In *Inorganic Electronic Structure and Spectroscopy*; Solomon, E. I., Lever, A. B. P., Eds.; Wiley: New York, 1999; Vol. 2, pp 403-450.

3. *Nitric Oxide: Biology and Pathobiology*; Ignarro, L., Ed.; Academic: San Diego, CA, 2000; pp 3-19.

4. Butler, A.; Nicholson, R. *Life, Death and Nitric Oxide*; The Royal Society of Chemistry: Cambridge, 2003.

5. *The Smallest Biomolecules: Diatomics and Their Interactions with Heme Proteins*; Ghosh, A., Ed.; Elsevier: Amsterdam, 2008, pp. 1-603.

6. Ghosh, A.; Hopmann, K. H.; Conradie, J. In *Computational Inorganic and Bioinorganic Chemistry*; Solomon, E. I., Scott, R. A. and King, R. B., Eds.; John Wiley & Sons, Ltd: Chichester, U.K., **2009**; pp 389– 410.

7 . For an introduction to DFT as applied to transition metal systems, see: Neese, F. *J. Biol. Inorg. Chem.* **2006**, *11*, 702-711.

8. For a biochemically oriented review, see: Noodleman, L.; Lovell, T.; Han, W.-H.; Li, J.; Himo, F. *Chem. Rev.* **2004**, *104*, 459–508

9. Hoffmann, R.; Chen, M. M. L.; Thorn, D. L. *Inorg. Chem.* **1977**, *16*, 503–511.

10. Enemark, J. H.; Feltham, R. D. *Coord. Chem. Rev.* **1974**, *13*, 339-406.

11. Ghosh, A. *Acc. Chem. Res.* **2005**, *38*, 943–954.

12. Li, M.; Bonnet, D.; Bill, E.; Neese, F.; Weyhermüller, T.; Blum, N.; Sellmann, D.; Wieghardt, K. *Inorg. Chem.* **2002**, *41*, 3444– 3456.

13. Garcia Serres, R., Grapperhaus, C. A., Bothe, E., Bill, E., Weyhermüller, T., Neese, F. and Wieghardt, K. *J. Am. Chem. Soc.* **2004**, *126*, 5138– 5153.

14. Tangen, E.; Conradie, J.; Svadberg, A.; Ghosh, A. *J. Inorg. Biochem.* **2005**, *99*, 55-59.

15. Conradie, J.; Quarless, D. A., Jr.; Hsu, H.-F.; Harrop, T. C.; Lippard, S. J.; Koch, S. A.; Ghosh, A. *J. Am. Chem. Soc.* **2007**, *129*, 10446–10456.

16. Conradie, J.; Ghosh, A. *J. Inorg. Biochem.* **2006**, *100*, 2069-2073.

17. Conradie, J.; Ghosh, A. *J. Phys. Chem. B* **2007**, *111*, 12621–12624.

18. Hopmann, K. H.; Ghosh, A.; Noodleman, L. *Inorg. Chem.* **2009**, *113*, 10540-10547.

19. Tangen, E.; Conradie, J.; Ghosh, A. *Inorg. Chem.* **2005**, *44*, 8699–8706.

20. Franz, K. J.; Lippard, S. J. *J. Am. Chem. Soc.* **1998**, *120*, 9034–9040.

21. (a) [Fe(5,5-TC)(NO)]: Franz, K. J.; Lippard, S. J. *J. Am. Chem. Soc.* **1999**, *121*, 10504–10512. (b) [Co(TC)(NO)]: K. J. Franz, L. H. Doerrer, B. Spingler and S. J. Lippard, *Inorg. Chem.*, 2001, **40**, 3774–3780.

22. Handy, N. C.; Cohen, A. J. *Mol. Phys.* **2001**, *99*, 403-412.

23. The LYP correlation functional: Lee, C., Yang, W., Parr, R. G. *Phys. Rev. B* **1988**, *37*, 785-789.

25. Reisner, E.; Telser, J.; Lippard, J. *Inorg. Chem.* **2007**, *46*, 10754-10770.

Abhik Ghosh 9/13/09 12:56 PM
Deleted: , 2001.

26. Boča, R. *Coord. Chem. Rev.* **2004**, *248*, 757-815.

27. Krzystek, J.; Telser, J. *J. Magn. Reson.* **2003**, *162*, 454-465.

28. Krzystek, J.; Telser, J.; Hoffman, B. M.; Brunel, L.-C.; Licoccia, S. *J. Am. Chem. Soc.* **2001**, *123*, 7890-7897.

29. Krzystek, J.; Telser, J.; Knapp, M. J.; Hendrickson, D. N.; Aromí, G.; Christou, G.; Angerhofer, A.; Brunel, L.-C. *Appl. Magn. Reson.* **2001**, *23*, 571-585.

30. Krzystek, J.; Telser, J.; Pardi, L. A.; Goldberg, D. P.; Hoffman, B. M.; Brunel, L.-C. *Inorg. Chem.* **1999**, *38*, 6121-6129.

31. Mossin, S.; Weihe, H.; Barra, A.-L. *J. Am. Chem. Soc.* **2002**, *124*, 8764-8765.

32. Barra, A.-L.; Gatteschi, D.; Sessoli, R.; Abbati, G. L.; Cornia, A.; Fabretti, A. C.; Uytterhoeven, M. G. *Angew. Chem. Int. Ed.* **1997**, *36*, 2329-2331.

33. Limburg, J.; Vrettos, J. S.; Crabtree, R. H.; Brudvig, G. W.; de Paula, J. C.; Hassan, A.; Barra, A.-L.; Duboc-Toia, C.; Collomb, M.-N. *Inorg. Chem.* **2001**, *40*, 1698-1703.

34. Krivokapic, I.; Noble, C.; Klitgaard, S.; Tregenna-Piggott, P. L. W.; Weihe, H.; Barra, A.-L. *Angew. Chem. Int. Ed.* **2005**, *44*, 3613-3616.

35. Hassan, A. K.; Pardi, L. A.; Krzystek, J.; Sienkiewicz, A.; Goy, P.; Rohrer, M.; Brunel, L.-C. *J. Magn. Reson.* **2000**, *142*, 300-312.

36. Ghosh, A.; Taylor, P. R. *Curr. Opin. Chem. Biol.* **2003**, *91*, 113-124.

37. Ghosh, A. *J. Biol. Inorg. Chem.* **2006**, *11*, 712– 724.

38. Swart, M. *J. Chem. Theory Comput.* **2008**, *4*, 2057-2066.

39. Conradie, J.; Ghosh, A. *J. Chem. Theory Comput.* **2007**, *3*, 689–702.

40. For recent corrections to the B3LYP functional, see: Rinaldo, D.; Tian, L.; Harvey, J. N.; Friesner, R. A. *J. Chem. Phys.* **2008**, *129*, Art. No. 164108.